Check for updates

Korean Journal of Radiology

KJR

Hepatocellular Carcinoma: Texture Analysis of Preoperative Computed Tomography Images Can Provide Markers of Tumor Grade and Disease-Free Survival

Jiseon Oh, MD[1, 2], Jeong Min Lee, MD[1-3], Junghoan Park, MD[1, 2], Ijin Joo, MD[1, 2], Jeong Hee Yoon, MD[1, 2], Dong Ho Lee, MD[1, 2], Balaji Ganeshan, PhD[4], Joon Koo Han, MD[1-3]

[1]Department of Radiology, Seoul National University Hospital, Seoul, Korea; [2]Department of Radiology, Seoul National University College of Medicine, Seoul, Korea; [3]Institute of Radiation Medicine, Seoul National University Medical Research Center, Seoul, Korea; [4]Institute of Nuclear Medicine, University College London, London, UK

Objective: To investigate the usefulness of computed tomography (CT) texture analysis (CTTA) in estimating histologic tumor grade and in predicting disease-free survival (DFS) after surgical resection in patients with hepatocellular carcinoma (HCC).
Materials and Methods: Eighty-one patients with a single HCC who had undergone quadriphasic liver CT followed by surgical resection were enrolled. Texture analysis of tumors on preoperative CT images was performed using commercially available software. The mean, mean of positive pixels (MPP), entropy, kurtosis, skewness, and standard deviation (SD) of the pixel distribution histogram were derived with and without filtration. The texture features were then compared between groups classified according to histologic grade. Kaplan-Meier and Cox proportional hazards analyses were performed to determine the relationship between texture features and DFS.
Results: SD and MPP quantified from fine to coarse textures on arterial-phase CT images showed significant positive associations with the histologic grade of HCC ($p < 0.05$). Kaplan-Meier analysis identified most CT texture features across the different filters from fine to coarse texture scales as significant univariate markers of DFS. Cox proportional hazards analysis identified skewness on arterial-phase images (fine texture scale, spatial scaling factor [SSF] 2.0, $p < 0.001$; medium texture scale, SSF 3.0, $p < 0.001$), tumor size ($p = 0.001$), microscopic vascular invasion ($p = 0.034$), rim arterial enhancement ($p = 0.024$), and peritumoral parenchymal enhancement ($p = 0.010$) as independent predictors of DFS.
Conclusion: CTTA was demonstrated to provide texture features significantly correlated with higher tumor grade as well as predictive markers of DFS after surgical resection of HCCs in addition to other valuable imaging and clinico-pathologic parameters.
Keywords: *Hepatocellular carcinoma; Computed tomography; Texture analysis; Recurrence; Disease-free survival; Prognosis*

INTRODUCTION

Hepatocellular carcinoma (HCC) is the second leading cause of cancer deaths worldwide (1). Hepatic resection is the preferred curative treatment option for early-stage HCCs in patients with good health and well-preserved liver function (2, 3). However, despite recent advances in surgical techniques, the high incidence of recurrence (up to 80%) remains a difficult challenge in the management of these patients (4). Thus, even after curative resection of HCC, patients are recommended to enroll in a surveillance program for the early detection of recurrence. However,

because the risk of recurrence is not uniform across all patients with HCCs, attempts have been made to determine risk factors for recurrence that can help identify high-risk patients. This high-risk group would undergo either intensive postoperative surveillance or radical treatment during the initial stages, potentially leading to improved outcomes. Therefore, identification of the risk factors for postoperative recurrence may be a crucial strategy for improving overall survival (OS) after surgical resection in patients with HCC.

For this purpose, various pathologic factors including tumor size; microscopic vascular invasion; satellite nodule; tumor, node, and metastasis stage; and histologic grade have been investigated and firmly established as risk factors of postoperative recurrence (5, 6). However, until now, no risk model capable of predicting HCC recurrence has been established, partly owing to the inability to obtain detailed, quantitative information of this heterogeneous tumor. Therefore, identification of more sophisticated and quantitative prognostic markers of HCC is clinically warranted.

Recently, radiomics has become another critical emerging area in oncology in addition to genomics and proteomics (7). In particular, texture analysis, which is a technique that can quantify the spatial pattern of pixel intensities on cross-sectional imaging, has been successfully applied to various types of cancers for the evaluation of tumor heterogeneity (8-14). Texture analysis has also been demonstrated to provide more information than visual inspection in an objective and quantitative manner regarding the biological aggressiveness of a tumor (13, 15). Furthermore, texture analysis in patients with malignant tumors has been demonstrated to provide information regarding not only tumor heterogeneity, but also histologic tumor grade, as well as predictive information regarding tumor recurrence or survival (16-21). However, until now, few studies have explored the value of computed tomography (CT) texture analysis (CTTA) in predicting disease-free survival (DFS) after surgical resection in patients with HCC (22). Therefore, the purpose of our study was to investigate the usefulness of CTTA in estimating the histologic tumor grade and in predicting DFS after surgical resection in patients with HCC.

MATERIALS AND METHODS

Patients

The Institutional Review Board of our institute approved this retrospective study and waived the requirement for
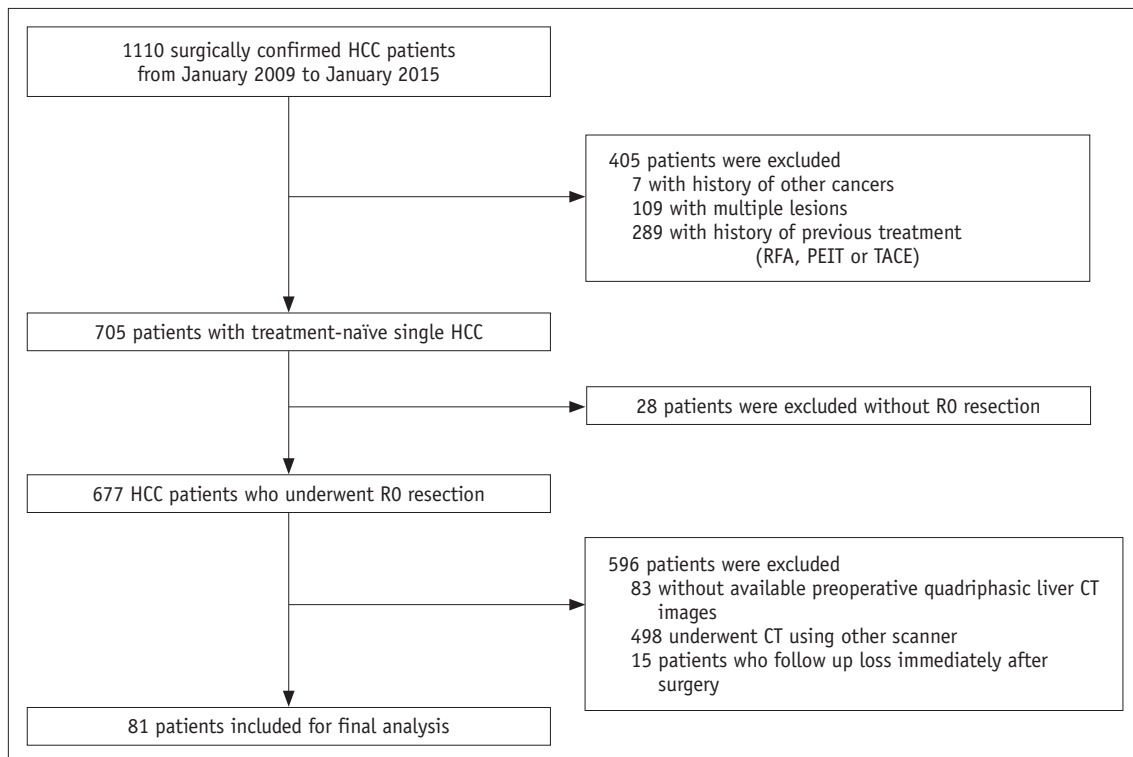

Fig. 1. Flowchart of inclusion and exclusion criteria. CT = computed tomography, HCC = hepatocellular carcinoma, PEIT = percutaneous ethanol injection therapy, RFA = radiofrequency ablation, TACE = trans-catheter arterial chemoembolization

informed consent. The study population consisted of patients diagnosed with HCC at a single center from January 2009 to January 2015 (Fig. 1). The inclusion criteria were as follows: 1) Patients with treatment-naïve single HCC; 2) patients who underwent R0 resection; 3) preoperative quadriphasic liver CT images (pre-contrast, arterial, portal-venous, and delayed phase) obtained less than 6 weeks before surgery; 4) follow-up of at least 2 years with no recurrence. The exclusion criteria were as follows: 1) Multiple lesions; 2) previous treatment with radiofrequency ablation (RFA), percutaneous ethanol injection therapy (PEIT), or trans-catheter arterial chemoembolization (TACE); 3) other accompanying cancers other than HCC; 4) CT using a protocol other than liver CT or a CT scanner other than a 64-detector row scanner (Brilliance 64, Philips Medical Systems, Cleveland, OH, USA); and 5) no available CT images reconstructed with filtered back projection. Finally, 81 patients, each with a single HCC and who had undergone quadriphasic contrast-enhanced CT using the same CT scanner comprised the study group (male:female, 65:16; mean age, 57.5 ± 10.8 years; age range 27–79 years).

CT Acquisition

In all study patients, CT examinations had been performed using a 64-detector row scanner (Brilliance 64) with the following scanning parameters: gantry rotation time of 0.5 seconds, 0.625 mm x 64-detector array, pitch of 1.0–1.5, table speed of 46.9 mm/rotation, 150–200 mAs, 120 kVp, and a 512 x 512 matrix. The reconstruction parameters were a 3-mm slice thickness and a 2- or 3-mm reconstruction interval. Arterial, portal-venous, and delayed phase CT images were obtained after administration of 1.5 mL/kg of a nonionic contrast material for 30 seconds (iohexol, Bonorex 350, Central Medical Service, Seoul, Korea; iobitridol, Xenetix 350, Guerbet, Aulnay-Sous-Bois, France) at a rate of 2.5–4.0 mL/s using a power injector. For arterial and portal-venous-phase scanning, 19- and 44-second delays were used after the maximal Hounsfield unit (HU) of the descending aorta reached 100 HU using bolus tracking. Delayed phase images were obtained 180 seconds after the start of contrast administration.

Imaging and Clinico-Pathologic Parameters

Preoperative CT images were retrospectively reviewed by one observer (a second-year resident of the Department of Radiology) under the supervision of an experienced abdominal radiologist (with 27 years of experience)

who were blinded to the clinico-pathologic information. Previously reported imaging features for the prediction of HCC recurrence, such as the presence of rim arterial enhancement, peritumoral parenchymal enhancement, and a non-smooth tumor margin, were evaluated for each HCC: 1) Peripheral rim arterial enhancement was defined as the presence of irregular ring-like areas of enhancement with central hypovascular areas on arterial-phase images (23); 2) peritumoral parenchymal enhancement was defined as gross hyper-enhancement outside of the tumor border regardless of shape on arterial-phase images (24); 3) tumor margins were classified as either smooth or non-smooth, with smooth tumor margins defined as a smooth tumor-normal

Table 1. Clinical Chracteristics of 81 Study Patients

Characteristics	Value
Age (years)	
Mean ± SD	57.5 ± 10.8
Sex, n (%)	
Males	65 (80.25)
Females	16 (19.75)
Etiology of liver cirrhosis, n (%)	
HBV-related	60 (74.07)
HCV-related	7 (8.64)
Alcoholic	3 (3.70)
Others	11 (13.58)
Child-Pugh score, n (%)	
5	78 (96.30)
6	2 (2.47)
7	1 (1.23)
BCLC staging, n (%)	
0	8 (9.88)
A	73 (90.12)
Size	
Mean ± SD	5.24 ± 3.71
Microscopic vascular invasion, n (%)	
Yes	29 (35.80)
No	52 (64.20)
Histologic grade, n (%)	
1	3 (3.70)
2	49 (60.49)
3	27 (33.33)
4	2 (2.47)
Serum AFP level (ng/mL)	
Mean ± SD	3324.30 ± 15000.84
Serum PIVKA-II level (ng/mL)	
Mean ± SD	5615.10 ± 14798.72

Continuous data expressed as mean ± SD. AFP = alpha-fetoprotein, BCLC = Barcelona Clinic Liver Cancer staging, HBV = hepatitis B virus, HCV = hepatitis C virus, PIVKA-II = vitamin K absence or antagonist-II, SD = standard deviation

liver interface on all axial, coronal, and sagittal images, and all other cases were considered non-smooth tumor margins (e.g., focal bulging, lobulating, or multinodular types) (25). In addition, the average attenuation of tumors (HU) was measured on arterial and portal-venous-phase images.

Histologic data of HCCs including tumor size, microvascular invasion, satellite nodule, and histological grade were retrieved from the histologic reports. Low-grade tumors corresponded to Edmondson grades I and II, and high-grade tumors corresponded to Edmondson grades III and IV (26). Other demographic and clinical data including age, sex, Child-Pugh score, Barcelona Clinic Liver Cancer stage, serum alpha-fetoprotein, and protein induced by Vitamin K absence or antagonist-II levels were also collected. The demographic, clinical, and pathological information are summarized in Table 1.

Texture Analysis

Arterial and portal-venous-phase liver CT images were assessed by two observers (second-year residents of the Department of Radiology), who were blinded to the clinico-pathologic information, using commercially available TexRAD software (TexRAD Ltd, Cambridge, UK) with the filtration-histogram method (27).

The technique comprised an initial filtration step in which a Laplacian of Gaussian spatial band-pass filter was used to selectively extract features of different sizes and intensity variations, followed by texture quantification (8, 27). The resultant images displayed features at different spatial scales from fine to coarse textures within a region of interest (ROI) drawn around the tumor (Fig. 2A). The scale was selected by tuning the filter parameter, also known as the spatial scaling factor (SSF), between 2.0 and 6.0. Each SSF corresponded to the same number of millimeters of pixels in radius, ranging from fine (SSF 2.0), to medium (SSF 3.0–5.0), to coarse (SSF 6.0) texture maps (9, 28). The ROI was delineated around the tumor outline at the level of the single largest cross-sectional area and further refined by excluding areas of fat, air, dense calcification, or bone; hence, the results included only pixels between 0 and 300 HU within the ROI (19). When the tumor margin was indistinct on arterial-phase images, the ROI was drawn after referencing the tumor margin on portal-venous or delayed phase images. Heterogeneity within this ROI was quantified with and without image filtration by calculating various texture parameters (mean, mean of positive pixels [MPP], entropy, kurtosis, skewness, and standard deviation [SD]) of

the pixel distribution histogram (Fig. 2B).

Follow-Up

Patients were followed-up until death or until March 2017 if they were still alive. Tumor recurrence was tracked at an outpatient clinic at least every 3–6 months using either tumor markers or imaging studies such as ultrasonography, CT, or magnetic resonance imaging. The onset of tumor recurrence was designated as the time at which a tumor was detected using one of these imaging techniques. DFS was defined as the time span from the date of surgery to the date of recurrence or the last clinical follow-up.

Statistical Analysis

All data were checked using the Shapiro-Wilk test for normality and the Levene test for equality of variance. The texture features of the largest cross-sectional area of the tumor were compared between groups of different histologic grades using Student's t test and multiple linear regression analysis was performed to determine variables independently associated with histologic grades. For Kaplan-Meier analysis, each parameter was dichotomized based on a cutpoint obtained using the minimum p value approach (29), and the two-fold cross validation approach was used to validate each cutpoint (30). Kaplan-Meier and Cox proportional hazards analyses were performed to determine the relationship between texture features on arterial/portal-venous-phase images and DFS. Interobserver agreement was measured using intraclass correlation coefficients (ICCs) for a randomly selected third of the study patients (27 of 81 patients). All statistical analyses were performed using commercially available software (MedCalc for Windows 17.6, MedCalc, Mariakerke, Belgium; SAS 9.4, SAS Institute Inc., Cary, NC, USA) with a p value of less than 0.05 considered to indicate a significant difference.

RESULTS

Patients

The mean follow-up period ± SD was 35.95 ± 26.14 months and the median follow-up was 32.6 months. Among the 81 study patients, 48 (59.3%) patients had recurrence and 33 (40.7%) patients had no recurrence during the follow-up period. Extrahepatic metastases developed in 5 of the 81 patients (6.2%), 11–50 months after HCC resection (median, 26.0 months). The locations of the initial extrahepatic metastases were the lung (n = 3), bone (n = 1),
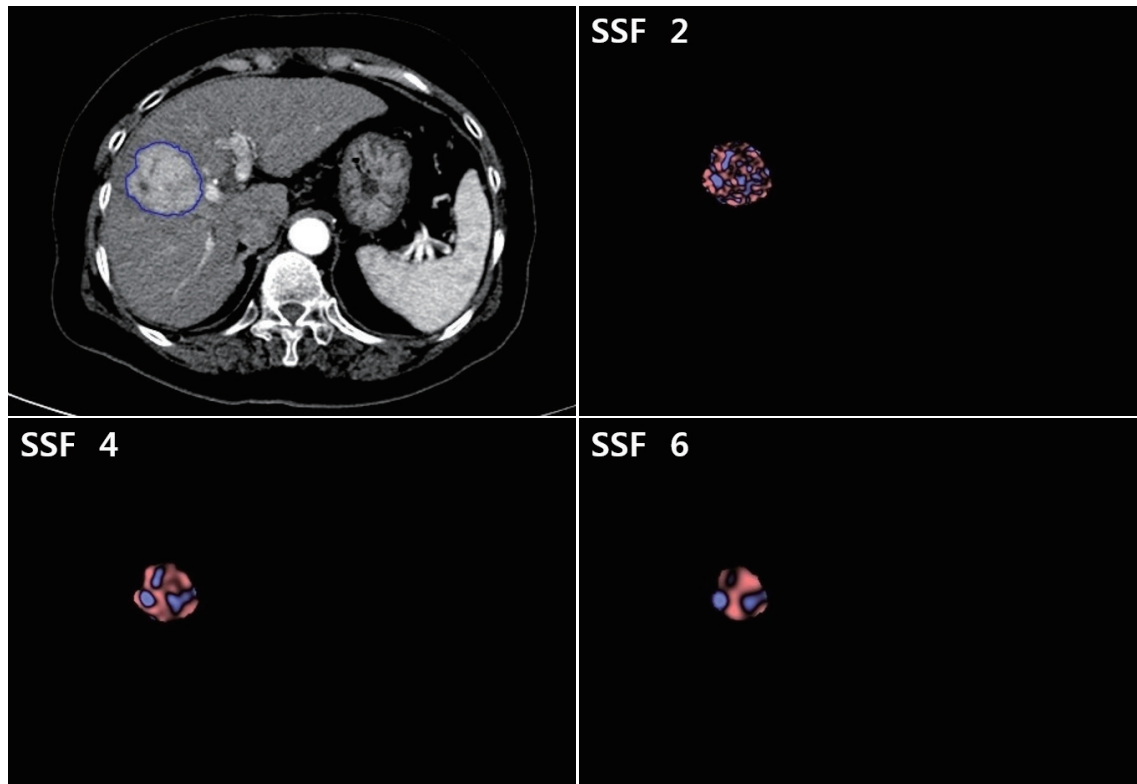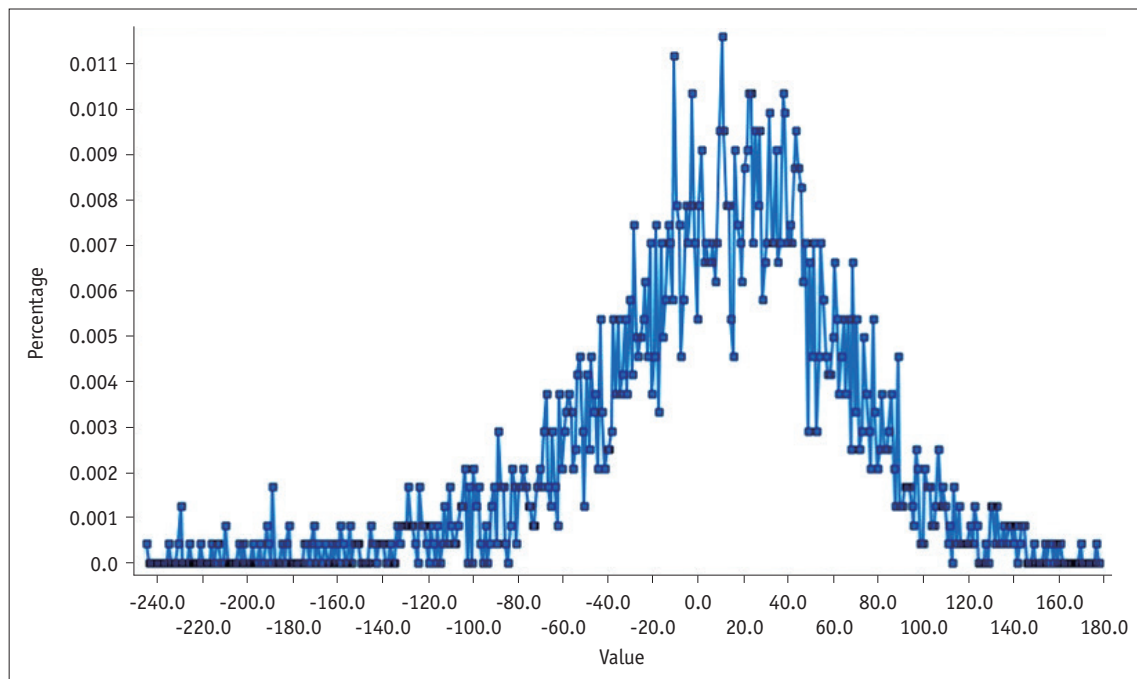
Fig. 2. Contrast-enhanced CT image of HCC in 64-year-old man with texture features.
A. CT image showing region of interest drawn around tumor (blue line) and corresponding images of fine, medium, and coarse textures obtained using filter values of 2, 4, and 6, respectively. **B.** Histogram derived from image showing pixel distribution at filter value of 2.0. SSF = spatial scaling factor

and adrenal gland (n = 1). Among these patients, four were treated with systemic chemotherapy, and the other with radiation therapy. Intrahepatic local recurrence developed in 4 of the 81 patients (4.9%), 24–46 months after HCC resection (median, 28.7 months) and intrahepatic distant recurrence developed in 39 of the 81 patients (48.2%), 2–66 months after HCC resection (median, 13.3 months). Among these patients, 31 were initially treated with TACE, 8 with RFA, 2 with PEIT, one with liver transplantation, and one with surgical resection to control the recurrent tumor. The median DFS time of the patients was 34.87 months (95% confidence interval, 24.80–66.47). The estimated 1-, 3-, and 5-year DFS rates after surgery were 72.5%, 48.7%, and

41.1%, respectively.

During the follow-up period, 16 of the 81 patients (19.7%) died. The estimated 1-, 3-, and 5-year OS rates after surgery were 72.5%, 48.7%, and 41.1%, respectively.

Texture Analysis

Correlation with the Histologic Grade of HCC

The texture parameters of the pixel distribution histogram on arterial and portal-venous-phase images are summarized in Tables 2 and 3. SD and MPP quantified from fine to coarse texture scales on arterial-phase CT images showed significant positive associations with the histologic grade of

Table 2. Texture Parameters of Pixel Distribution Histogram without Filtration and with Filtration on Arterial-Phase

Filter Scale Values	Mean	SD	Entropy	MPP	Skewness	Kurtosis
No filtration	81.79 ± 20.04	21.65 ± 4.88	4.40 ± 0.23	81.79 ± 20.04	0.29 ± 0.53	0.69 ± 2.21
2.0 (fine)	6.32 ± 9.55	49.17 ± 12.36	5.56 ± 4.52	41.17 ± 10.65	0.26 ± 0.58	1.69 ± 6.09
3.0 (medium)	7.22 ± 12.36	43.88 ± 14.49	4.79 ± 0.86	38.02 ± 13.48	0.80 ± 5.47	1.11 ± 3.48
4.0 (medium)	8.78 ± 18.71	39.51 ± 17.74	4.66 ± 0.89	36.80 ± 15.49	0.20 ± 0.87	1.21 ± 5.75
5.0 (medium)	8.32 ± 20.45	36.43 ± 19.61	4.90 ± 4.31	34.88 ± 17.81	0.55 ± 3.92	0.41 ± 3.45
6.0 (coarse)	9.41 ± 17.51	33.87 ± 20.51	4.16 ± 1.56	33.19 ± 18.14	0.11 ± 0.56	0.10 ± 2.69

Continuous data expressed as mean ± SD. MPP = mean of positive pixels

Table 3. Texture Parameters of Pixel Distribution Histogram without Filtration and with Filtration on Portal-venous-Phase

Filter Scale Values	Mean	SD	Entropy	MPP	Skewness	Kurtosis
No filtration	94.67 ± 18.41	20.30 ± 5.18	4.33 ± 0.26	94.67 ± 18.41	-0.08 ± 0.35	0.44 ± 0.76
2.0 (fine)	-1.38 ± 4.67	44.83 ± 10.48	4.99 ± 0.38	35.06 ± 8.65	0.00 ± 0.29	0.28 ± 0.66
3.0 (medium)	-1.74 ± 8.47	37.99 ± 13.47	4.76 ± 0.53	29.23 ± 11.57	-0.12 ± 0.45	0.40 ± 0.94
4.0 (medium)	-2.60 ± 11.65	34.26 ± 15.39	4.54 ± 0.78	26.39 ± 12.75	-0.13 ± 0.61	0.16 ± 1.37
5.0 (medium)	-3.68 ± 13.77	30.91 ± 17.04	4.28 ± 1.17	23.61 ± 13.68	-0.13 ± 0.60	0.38 ± 1.55
6.0 (coarse)	-4.64 ± 14.94	28.09 ± 18.26	4.00 ± 1.53	21.05 ± 14.70	-0.16 ± 0.58	0.25 ± 1.34

Continuous data expressed as mean ± SD.

Table 4. Comparison of Texture Parameters between High-Grade and Low-Grade HCCs on Arterial-Phase

Filter Scale Values	Mean	SD	Entropy
No filtration	0.62 (-8.68–9.92, 0.895)	1.86 (-0.37–4.09, 0.100)	0.08 (-0.03–0.19, 0.147)
2.0 (fine)	-0.70 (-5.13–3.73, 0.754)	6.69 (1.15–12.23, 0.019)	-0.68 (-2.77–1.41, 0.519)
3.0 (medium)	0.79 (-4.99–6.57, 0.786)	8.27 (2.17–14.38, 0.009)	0.20 (-0.11–0.52, 0.196)
4.0 (medium)	1.15 (-7.61–9.91, 0.795)	11.10 (3.45–18.76, 0.005)	0.19 (-0.14–0.53, 0.257)
5.0 (medium)	2.10 (-7.72–11.91, 0.672)	12.83 (4.53–21.13, 0.003)	-0.44 (-2.46–1.59, 0.669)
6.0 (coarse)	-0.35 (-8.97–8.27, 0.936)	10.70 (2.04–19.36, 0.016)	0.10 (-0.41–0.60, 0.707)
Filter Scale Values	MPP	Skewness	Kurtosis
No filtration	0.62 (-8.68–9.92, 0.895)	0.15 (-0.09–0.39, 0.225)	-0.08 (-1.11–0.94, 0.872)
2.0 (fine)	4.72 (-0.11–9.55, 0.045)	0.07 (-0.20–0.34, 0.611)	-0.36 (-3.19–2.46, 0.798)
3.0 (medium)	6.58 (0.77–12.39, 0.027)	-0.79 (-3.35–1.77, 0.541)	0.07 (-1.57–1.70, 0.936)
4.0 (medium)	8.88 (2.17–15.58, 0.010)	-0.02 (-0.43–0.39, 0.930)	-0.88 (-3.57–1.81, 0.515)
5.0 (medium)	11.44 (3.96–18.92, 0.003)	-0.70 (-2.58–1.18, 0.463)	-0.26 (-1.92–1.40, 0.755)
6.0 (coarse)	9.94 (2.58–17.29, 0.009)	-0.02 (-0.30–0.26, 0.906)	-0.23 (-1.57–1.11, 0.731)

Mean difference (95% CI, *p* value). CI = confidence interval, HCC = hepatocellular carcinoma

the tumors ($p < 0.05$); high-grade HCCs showed significantly higher MPP and SD than low-grade HCCs at all texture scales on CTTA of arterial-phase CT images (Table 4). However, no significant differences in texture parameters were observed ($p > 0.05$) between low-grade and high-grade tumors at all filter levels on portal-venous-phase CT images (Table 5). Multiple linear regression analysis revealed that SD and MPP of medium texture scales on arterial-phase images showed an independently significant correlation with the histologic grade of HCC (SD at SSF 4.0, B = 0.009, $p = 0.005$; MPP at SSF 4.0, B = 0.012, $p = 0.013$).

Relationship between CTTA and DFS

Univariate analysis identified most CT texture parameters across the different filters of fine, medium, and coarse texture scales as significant univariate markers of DFS (Supplementary Tables 1, 2 in the online-only Data Supplement) (Fig. 3). In addition, numerous previously reported imaging and clinico-pathologic features were demonstrated to be significant univariate markers of DFS (Supplementary Table 3 in the online-only Data Supplement). The multivariate analysis, which included all significant univariate markers among the arterial-phase texture parameters and other imaging/clinico-pathological features, identified skewness on arterial-phase images (fine texture scale, SSF 2.0, $p < 0.001$; medium texture scale, SSF 3.0, $p < 0.001$), tumor size ($p = 0.001$), microscopic vascular invasion ($p = 0.034$), rim arterial enhancement ($p = 0.024$), and peritumoral parenchymal enhancement ($p = 0.010$) as independent predictors of DFS (Table 6). Furthermore, the multivariate analysis, which included all significant univariate markers among the portal-venous-phase texture parameters and other imaging/clinico-pathological features, identified that tumor size ($p < 0.001$),

Table 5. Comparison of Texture Parameters between High-Grade and Low-Grade HCCs on Portal-venous-Phase

Filter Scale Values	Mean	SD	Entropy
No filtration	-4.26 (-12.75–4.23, 0.321)	0.98 (-1.41–3.38, 0.415)	0.05 (-0.07–0.17, 0.403)
2.0 (fine)	0.32 (-1.85–2.48, 0.773)	0.62 (-4.24–5.49, 0.799)	0.01 (-0.16–0.19, 0.888)
3.0 (medium)	0.11 (-3.83–4.04, 0.956)	0.53 (-5.73–6.78, 0.867)	0.04 (-0.21–0.29, 0.741)
4.0 (medium)	-0.09 (-5.50–5.32, 0.974)	1.39 (-5.75–8.53, 0.699)	0.04 (-0.33–0.40, 0.840)
5.0 (medium)	-0.20 (-6.65–6.26, 0.951)	2.59 (-5.21–10.39, 0.510)	-0.07 (-0.57–0.43, 0.779)
6.0 (coarse)	-2.46 (-10.08–5.16, 0.522)	5.88 (-2.24–14.00, 0.153)	0.11 (-0.35–0.56, 0.632)
Filter Scale Values	MPP	Skewness	Kurtosis
No filtration	-4.26 (-12.75–4.23, 0.321)	0.09 (-0.07–0.25, 0.272)	-0.37 (-0.71–-0.03, 0.033)
2.0 (fine)	1.25 (-2.75–5.26, 0.535)	0.13 (0.00–0.26, 0.057)	0.03 (-0.28–0.34, 0.839)
3.0 (medium)	0.65 (-4.72–6.01, 0.812)	0.07 (-0.13–0.28, 0.479)	-0.20 (-0.63–0.24, 0.371)
4.0 (medium)	1.47 (-4.45–7.38, 0.623)	0.06 (-0.23–0.34, 0.690)	-0.31 (-0.94–0.33, 0.339)
5.0 (medium)	3.17 (-3.08–9.43, 0.315)	0.13 (-0.15–0.41, 0.368)	-0.15 (-0.88–0.57, 0.672)
6.0 (coarse)	4.15 (-2.54–10.84, 0.220)	0.18 (-0.11–0.47, 0.220)	-0.35 (-1.03–0.34, 0.315)

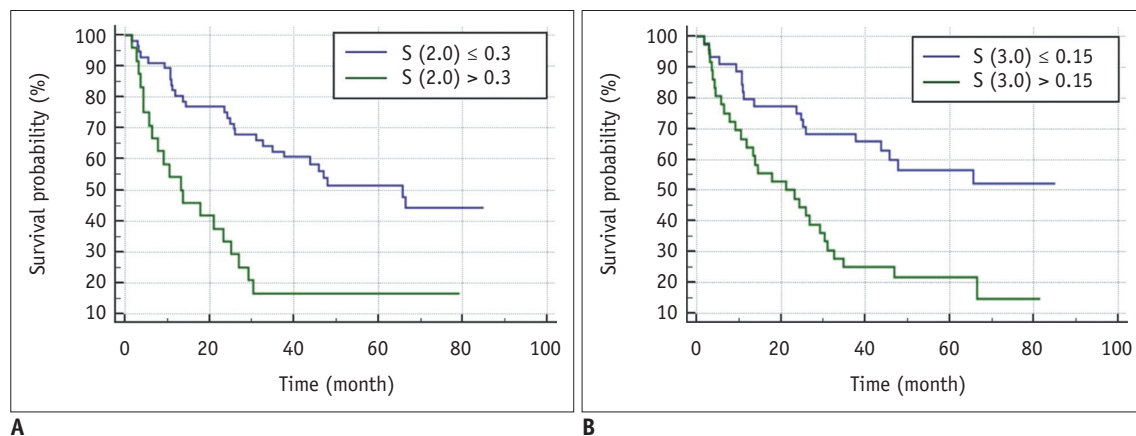Mean difference (95% CI, p value).

Fig. 3. Kaplan-Meier curves on arterial-phase CT images showing significant difference in disease-free survival for (A) skewness at spatial scaling factors of 2.0 and (B) 3.0 with p values of < 0.001 and < 0.001, respectively.

Table 6. Multivariate Analysis of Texture Parameters on Arterial-Phase and Other Imaging/Clinico-Pathological Features for DFS

Characteristic	Hazard Ratio	95% CI	P
Skewness (SSF 2.0)	10.96	3.21–37.46	< 0.001
Skewness (SSF 3.0)	1.90	1.35–2.67	< 0.001
Size	1.30	1.12–1.51	0.001
Microscopic vascular invasion	2.12	1.06–4.25	0.034
Rim arterial enhancement	3.35	1.17–9.56	0.024
Peritumoral parenchymal enhancement	3.18	1.32–7.64	0.010

DFS = disease-free survival, SSF = spatial scaling factor

Table 7. Multivariate Analysis of Texture Parameters on Portal-venous-Phase and Other Imaging/Clinico-Pathological Features for DFS

Characteristic	Hazard Ratio	95% CI	P
Size	1.22	1.14–1.31	< 0.001
Satellite nodule	5.70	1.54–21.12	0.009
Rim arterial enhancement	3.33	1.27–8.69	0.014

satellite nodule (*p* = 0.009), and rim arterial enhancement (*p* = 0.014) were separately independent predictors of DFS (Table 7).

Interobserver Agreement

Most CT texture features across the different filters of fine, medium, and coarse texture scales showed good to excellent interobserver agreement based on the ICCs of the readers (Supplementary Tables 4, 5 in the online-only Data Supplement) (31).

DISCUSSION

Our study demonstrated that SD and MPP quantified from fine to coarse texture scales on arterial-phase CT images showed significant associations with the histologic grade of HCCs after surgical resection. In addition, multivariate analysis identified skewness on arterial-phase CT images (fine and medium texture scales), tumor size, microscopic vascular invasion, rim arterial enhancement, and peritumoral parenchymal enhancement as independent predictors of DFS. Therefore, considering that CTTA is only an additional post-processing tool that analyzes existing CT images without additional radiation exposure to the patient, CTTA features may be used as imaging-based predictive markers of DFS that can reflect the heterogeneity of HCC, which is a well-known feature of malignancy (32). Previous studies have already demonstrated that CTTA parameters

may be used as significant predictive markers of survival in other malignant tumors such as non-small cell lung cancer, esophageal cancer, colorectal cancer, renal cell carcinoma, and glioma (12, 15-17, 33) and our study results are in close agreement with the results of these studies.

In our study, high-grade HCCs showed significantly higher SD and MPP on CTTA of arterial-phase CT images than low-grade HCCs at all texture scales. In CTTA, MPP values only account for pixels greater than 0 and SD values increase with dark or bright objects highlighted by the filter. Therefore, the positive association between the histologic grade of HCCs and MPP/SD reflects the predominance of bright areas on arterial-phase images of tumors with high angiogenesis (27). According to a previous study, when the texture is coarse, heterogeneity is ascribed predominantly to the heterogeneity of the tumor vascular supply, whereas when the texture is fine, texture features also reflect the distribution of the contrast agent between intra- and extravascular extracellular spaces, which may be related to altered permeability (20). Thus, CTTA parameters at various settings may reflect the heterogeneity of tumor vascularity as well as higher permeability. During hepatocarcinogenesis, the normal portal vein and hepatic artery apparently decrease and abnormal intratumoral arterioles develop because of tumor angiogenesis (34). These changes in the blood supply of HCCs create the different patterns of enhancement in the two phases of dynamic contrast-enhanced CT (35-38), which can affect the image texture on contrast-enhanced CT, and CTTA may be able to represent these vascular changes.

We also found that skewness on arterial-phase CT images was an independent predictor of DFS in patients with HCC. More specifically, multivariate analysis identified that skewness greater than 0.3 at SSF 2.0 and skewness greater than 0.15 at SSF 3.0 was associated with poorer DFS. Increased skewness may reflect the average brightness of highlighted objects (blood vessels) (27). Therefore, our results suggest that HCCs with high angiogenesis and variation in vascular permeability may have worse DFS (20). Several studies have demonstrated that in patients with malignant tumors, CTTA could provide predictive information regarding tumor progression or survival. In a study that assessed 57 patients with colorectal cancer, fine texture features of CTTA within the whole tumor were demonstrated to be associated with a poorer 5-year OS rate (20). In addition, other studies focusing on hepatic texture in patients with colorectal cancer have demonstrated that higher heterogeneity of coarse

liver texture may be related to the presence of occult malignancies and a poorer prognosis (9, 19). Therefore, our study results suggest that CTTA may provide a useful adjunct to known clinico-pathologic markers, improving the stratification of HCC patients for risk of recurrence, thereby allowing more appropriate modification of surveillance strategies for specific subgroups with a high risk of recurrence.

Notably, our study differed from previously published studies in several aspects. First, we used contrast-enhanced CT images for CTTA rather than unenhanced CT images. Previous studies have shown significant differences in texture features between unenhanced and contrast-enhanced CT images (39). However, we surmised that the pathological changes of HCC could be more clearly depicted on contrast-enhanced CT rather than unenhanced CT images. Second, we included both arterial-phase and portal-venous-phase images for CTTA, whereas most previous studies have used only portal-venous-phase images. As mentioned, considering that HCCs have different patterns of enhancement in the two phases of dynamic contrast-enhanced liver CT, CTTA of both arterial-phase and portal-venous-phase images may be more appropriate than CTTA of portal-venous-phase images alone.

Nevertheless, this study had several limitations. First, the retrospective study design may have created the potential for bias. Previous studies have indicated that the reproducibility and variability of texture analysis is affected by CT vendors, acquisition parameters including acquisition time, and reconstruction methods. Therefore, we included 81 patients who underwent contrast-enhanced CT using the same quadriphasic protocol performed with the same CT scanner. This may have led to a slightly more limited sample size, and even when using the same quadriphasic protocol, the timing of image acquisition can vary slightly from image to image, thus affecting texture analysis results. Therefore, additional studies with a larger number of cases and image processing techniques such as normalization are warranted to apply the study results to other CT vendors. Second, texture analysis in our study was performed in a limited tumor area rather than the whole tumor. However, several previous studies using texture analysis of only the largest cross-sectional area were still able to demonstrate its promise as a predictive biomarker (16-18). Nonetheless, additional studies using whole tumor analysis for HCCs are warranted based on a previous investigation that demonstrated that the separation of the Kaplan-Meier curve

for 5-year OS with whole tumor analysis was superior to that with single-slice analysis (40).

In conclusion, CTTA was demonstrated to provide texture features significantly correlated with higher tumor grade as well as predictive markers of DFS in patients with HCC in addition to other valuable imaging and clinico-pathologic parameters. If additional studies including whole tumor analysis can validate our results, CTTA has the potential to become a highly useful quantitative biomarker in the management of patients with HCC.

Supplementary Materials

The online-only Data Supplement is available with this article at https://doi.org/10.3348/kjr.2018.0501.

Conflicts of Interest

The authors have no potential conflicts of interest to disclose.

ORCID iDs

Jeong Min Lee
    https://orcid.org/0000-0003-0561-8777
Jiseon Oh
    https://orcid.org/0000-0002-2516-2589

REFERENCES

1. Ferlay J, Soerjomataram I, Dikshit R, Eser S, Mathers C, Rebelo M, et al. Cancer incidence and mortality worldwide: sources, methods and major patterns in GLOBOCAN 2012. *Int J Cancer* 2015;136:E359-E386
2. Bruix J, Sherman M; American Association for the Study of Liver Diseases. Management of hepatocellular carcinoma: an update. *Hepatology* 2011;53:1020-1022
3. European Association For The Study Of The Liver; European Organisation For Research And Treatment Of Cancer. EASL-EORTC clinical practice guidelines: management of hepatocellular carcinoma. *J Hepatol* 2012;56:908-943
4. Takayama T, Makuuchi M, Hirohashi S, Sakamoto M, Yamamoto J, Shimada K, et al. Early hepatocellular carcinoma as an entity with a high rate of surgical cure. *Hepatology* 1998;28:1241-1246
5. Poon RT, Fan ST, Ng IO, Lo CM, Liu CL, Wong J. Different risk factors and prognosis for early and late intrahepatic recurrence after resection of hepatocellular carcinoma. *Cancer* 2000;89:500-507
6. Imamura H, Matsuyama Y, Tanaka E, Ohkubo T, Hasegawa K, Miyagawa S, et al. Risk factors contributing to early and late phase intrahepatic recurrence of hepatocellular carcinoma

after hepatectomy. *J Hepatol* 2003;38:200-207

7. Gillies RJ, Kinahan PE, Hricak H. Radiomics: images are more than pictures, they are data. *Radiology* 2016;278:563-577

8. Miles KA, Ganeshan B, Hayball MP. CT texture analysis using the filtration-histogram method: what do the measurements mean? *Cancer Imaging* 2013;13:400-406

9. Ganeshan B, Miles KA, Young RC, Chatwin CR. Texture analysis in non-contrast enhanced CT: impact of malignancy on texture in apparently disease-free areas of the liver. *Eur J Radiol* 2009;70:101-110

10. Zhou W, Zhang L, Wang K, Chen S, Wang G, Liu Z, et al. Malignancy characterization of hepatocellular carcinomas based on texture analysis of contrast-enhanced MR images. *J Magn Reson Imaging* 2017;45:1476-1484

11. Shimizu K, Yamada K, Noda K. [Computed tomography analysis of resected small adenocarcinomas of the lung less than 15 mm in diameter--correlation of radiologic and histologic characteristics]. *Nihon Kokyuki Gakkai Zasshi* 1998;36:672-678

12. Skogen K, Ganeshan B, Good C, Critchley G, Miles K. Measurements of heterogeneity in gliomas on computed tomography relationship to tumour grade. *J Neurooncol* 2013;111:213-219

13. Ganeshan B, Ziauddin Z, Goh V, Rodriguez-Justo M, Engledow A, Taylor S, et al. Quantitative imaging biomarkers from PET-CT as potential correlates for angiogenesis and hypoxia in colorectal cancer. *European Society of Radiology* 2012 [Epub]. https://doi.org/10.1594/ecr2012/B-0876

14. Sahiner B, Chan HP, Petrick N, Helvie MA, Goodsitt MM. Computerized characterization of masses on mammograms: the rubber band straightening transform and texture analysis. *Med Phys* 1998;25:516-526

15. Ganeshan B, Goh V, Mandeville HC, Ng QS, Hoskin PJ, Miles KA. Non-small cell lung cancer: histopathologic correlates for texture parameters at CT. *Radiology* 2013;266:326-336

16. Goh V, Ganeshan B, Nathan P, Juttla JK, Vinayan A, Miles KA. Assessment of response to tyrosine kinase inhibitors in metastatic renal cell cancer: CT texture as a predictive biomarker. *Radiology* 2011;261:165-171

17. Ganeshan B, Skogen K, Pressney I, Coutroubis D, Miles K. Tumour heterogeneity in oesophageal cancer assessed by CT texture analysis: preliminary evidence of an association with tumour metabolism, stage, and survival. *Clin Radiol* 2012;67:157-164

18. Zhang H, Graham CM, Elci O, Griswold ME, Zhang X, Khan MA, et al. Locally advanced squamous cell carcinoma of the head and neck: CT texture and histogram analysis allow independent prediction of overall survival in patients treated with induction chemotherapy. *Radiology* 2013;269:801-809

19. Miles KA, Ganeshan B, Griffiths MR, Young RC, Chatwin CR. Colorectal cancer: texture analysis of portal phase hepatic CT images as a potential marker of survival. *Radiology* 2009;250:444-452

20. Ng F, Ganeshan B, Kozarski R, Miles KA, Goh V. Assessment of primary colorectal cancer heterogeneity by using whole-tumor

21. Yu H, Caldwell C, Mah K, Mozeg D. Coregistered FDG PET/CT-based textural characterization of head and neck cancer for radiation treatment planning. *IEEE Trans Med Imaging* 2009;28:374-383

22. Chen S, Zhu Y, Liu Z, Liang C. Texture analysis of baseline multiphasic hepatic computed tomography images for the prognosis of single hepatocellular carcinoma after hepatectomy: a retrospective pilot study. *Eur J Radiol* 2017;90:198-204

23. An C, Kim DW, Park YN, Chung YE, Rhee H, Kim MJ. Single hepatocellular carcinoma: preoperative MR imaging to predict early recurrence after curative resection. *Radiology* 2015;276:433-443

24. Kim H, Park MS, Choi JY, Park YN, Kim MJ, Kim KS, et al. Can microvessel invasion of hepatocellular carcinoma be predicted by pre-operative MRI? *Eur Radiol* 2009;19:1744-1751

25. Chou CT, Chen RC, Lin WC, Ko CJ, Chen CB, Chen YL. Prediction of microvascular invasion of hepatocellular carcinoma: preoperative CT and histopathologic correlation. *AJR Am J Roentgenol* 2014;203:W253-W259

26. Edmondson HA, Steiner PE. Primary carcinoma of the liver: a study of 100 cases among 48,900 necropsies. *Cancer* 1954;7:462-503

27. Miles KA, Ganeshan B, Hayball MP. CT texture analysis using the filtration-histogram method: what do the measurements mean? *Cancer Imaging* 2013;13:400-406

28. Lubner MG, Malecki K, Kloke J, Ganeshan B, Pickhardt PJ. Texture analysis of the liver at MDCT for assessing hepatic fibrosis. *Abdom Radiol (NY)* 2017;42:2069-2078

29. Williams BA, Mandrekar JN, Mandrekar SJ, Cha SS, Furth AF. *Finding optimal cutpoints for continuous covariates with binary and time-to-event outcomes (Technical Report Series #79)*. Rochester, MN: Mayo Foundation, 2006

30. Faraggi D, Simon R. A simulation study of cross-validation for selecting an optimal cutpoint in univariate survival analysis. *Stat Med* 1996;15:2203-2213

31. Cicchetti DV. Guidelines, criteria, and rules of thumb for evaluating normed and standardized assessment instruments in psychology. *Psychol Assess* 1994;6:284-290

32. Nelson DA, Tan TT, Rabson AB, Anderson D, Degenhardt K, White E. Hypoxia and defective apoptosis drive genomic instability and tumorigenesis. *Genes Dev* 2004;18:2095-2107

33. Lubner MG, Stabo N, Lubner SJ, del Rio AM, Song C, Halberg RB, et al. CT textural analysis of hepatic metastatic colorectal cancer: pre-treatment tumor heterogeneity correlates with pathology and clinical outcomes. *Abdom Imaging* 2015;40:2331-2337

34. Nakashima Y, Nakashima O, Hsia CC, Kojiro M, Tabor E. Vascularization of small hepatocellular carcinomas: correlation with differentiation. *Liver* 1999;19:12-18

35. Efremidis SC, Hytiroglou P. The multistep process of hepatocarcinogenesis in cirrhosis with imaging correlation.

Eur Radiol 2002;12:753-764

36. Kitao A, Zen Y, Matsui O, Gabata T, Nakanuma Y. Hepatocarcinogenesis: multistep changes of drainage vessels at CT during arterial portography and hepatic arteriography--radiologic-pathologic correlation. *Radiology* 2009;252:605-614

37. Hayashi M, Matsui O, Ueda K, Kawamori Y, Kadoya M, Yoshikawa J, et al. Correlation between the blood supply and grade of malignancy of hepatocellular nodules associated with liver cirrhosis: evaluation by CT during intraarterial injection of contrast medium. *AJR Am J Roentgenol* 1999;172:969-976

38. Choi JY, Lee JM, Sirlin CB. CT and MR imaging diagnosis and staging of hepatocellular carcinoma: part I. Development, growth, and spread: key pathologic and imaging aspects. *Radiology* 2014;272:635-654

39. Kiryu S, Akai H, Nojima M, Hasegawa K, Shinkawa H, Kokudo N, et al. Impact of hepatocellular carcinoma heterogeneity on computed tomography as a prognostic indicator. *Sci Rep* 2017;7:12689

40. Ng F, Kozarski R, Ganeshan B, Goh V. Assessment of tumor heterogeneity by CT texture analysis: can the largest cross-sectional area be used as an alternative to whole tumor analysis? *Eur J Radiol* 2013;82:342-348